CrossMark
click for updates

The non-dominance of counterions in charge-asymmetric electrolytes: non-monotonic precedence of electrostatic screening and local inversion of the electric field by multivalent coions

Guillermo Iván Guerrero-García,*[a] Enrique González-Tovar,[b]
Manuel Quesada-Pérez[c] and Alberto Martín-Molina[d]

The asymptotic convergence of the thermodynamic and structural properties of unequally-sized charge-symmetric ions in strong electric fields was postulated more than thirty years ago by Valleau and Torrie as the dominance of counterions *via* the non-linear Poisson–Boltzmann theory [Valleau and Torrie, *J. Chem. Phys.*, 1982, **76**, 4623]. According to this mean field prescription, the properties of the electrical double layer near a highly charged electrode immersed in a size-asymmetric binary electrolyte converge to those of a size-symmetric electrolyte if the properties of counterions are the same in both instances. On the other hand, some of the present authors have shown that, in fact, counterions do not dominate the electrical properties of a spherical macroion in the presence of unequally-sized ions, symmetric in valence, if ion correlations and ionic excluded volume effects are taken into account consistently. These ingredients are neglected in the classical Poisson–Boltzmann picture. In the present work, we show the occurrence of the non-dominance of counterions in the opposite scenario, that is, when ions are equally-sized but asymmetric in valence. This is performed in the presence of highly charged colloidal surfaces of spherical and planar geometries for different ionic volume fractions. In addition to the phenomenon of non-dominance of counterions, our simulations and theoretical data also exhibit a non-monotonic order or precedence in the mean electrostatic potential, or electrostatic screening, at the Helmholtz plane of a charged colloid. This interesting behaviour is analyzed as a function of the coion's valence, the ionic volume fraction, and the charge and size of the colloidal particle. All these phenomena are explained in terms of the decay of the electric field near the colloidal surface, and by the appearance of a local inversion of both the electric field and the integrated surface charge density of the colloidal particle in the presence of monovalent counterions and multivalent coions.

1 Introduction

Due to its unquestionable relevance in colloid science, the attainment of a correct description of the ionic cloud surrounding charged surfaces in solution, *i.e.*, the so-called electrical double layer, has convoked a great deal of theoretical, experimental,

and simulation effort since the last century. As a result of this collective endeavour, a clearer picture of this physico-chemical charge distribution has recently emerged. In spite of these advances, several interesting and counterintuitive new phenomena, which includes the local charge reversal and surface charge amplification of colloids,[1–5] have much revivified the study of the electrical double layer in recent years.[6–22] Thus, we can realize that, even if a fundamental understanding of the electrical double layer has already been established, there is still space for new knowledge and refinements in relation to this concept.

In 1982, Valleau and Torrie performed a theoretical study of the role of the ionic size-asymmetry in the charge distribution of a binary mixture of semi-punctual ions, symmetric in valence, next to a charged plane.[23] In that Poisson–Boltzmann work, they enunciated an apparently "obvious" or expected fact later known

[a] CONACYT – Instituto de Física de la Universidad Autónoma de San Luis Potosí,
Álvaro Obregón 64, 78000 San Luis Potosí, San Luis Potosí, Mexico.
E-mail: givan@ifisica.uaslp.mx; Tel: +52 444 8262300, ext. 5723
[b] Instituto de Física de la Universidad Autónoma de San Luis Potosí,
Álvaro Obregón 64, 78000 San Luis Potosí, San Luis Potosí, Mexico
[c] Departamento de Física, Universidad de Jaén,
Escuela Politécnica Superior de Linares, 23700 Linares, Jaén, Spain
[d] Grupo de Física de Fluidos y Biocoloides, Departamento de Física Aplicada,
Facultad de Ciencias, Universidad de Granada, 18071 Granada, Spain

as the dominance of the counterions in the electrical double layer. According to these authors, only counterions are found near the surface of a strongly charged colloid of either sign. Thus, in the limit of strong electric fields, the ionic size-asymmetry between coions and counterions becomes irrelevant and the only important ion-size parameter is the effective radius of the counterions. In other words, and quoting those authors: "...When there is a substantial surface charge...we expect the double layer properties of a dilute electrolyte to become similar to those of a completely symmetric electrolyte having an effective size equal to that of the counterion...". In such a scenario, the contribution of coions to the properties of the diffuse electrical double layer becomes negligible regarding the contribution of counterions. As a result, the properties and behaviour of coions at large electric fields are irrelevant in this classic description of the electrical double layer, whose characteristics are dominated or determined mainly by counterions. It must be stressed that this appealing dominance idea was proved to be asymptotically exact for large fields only in the non-linear Poisson–Boltzmann theory of semi-punctual electrolytes asymmetric in size and symmetric in valence.[23]

Note that in the semi-punctual model of the electrical double layer introduced by Valleau and Torrie the electrolytic bath is constituted by ions with a dual character, *i.e.*, these ions interact between them as point charges but they act as charged hard spheres (with different closest approach distances for counterions and coions) with respect to a planar electrode. Therefore, this semi-punctual representation of the electrolyte can be considered as the lowest-order way to incorporate ion-size effects in the electrical double layer treatment.

Interestingly, Barrios-Contreras *et al.*[24] have reported very recently a complementary phenomenon to the dominance of counterions at large electric fields in the non-linear Poisson–Boltzmann theory, but this time associated with non-highly charged colloids immersed in a binary mixture of semi-punctual electrolytes asymmetric in valence and size. In that work it has also been demonstrated that, for a given ionic size-asymmetry, a fixed concentration of the smallest ionic species, and weakly/moderate colloidal surface charges, the valence of small ions rules or mainly determines the thermodynamic and structural properties of the electrical double layer regardless of the polarity of the charged colloid. In other words, according to the non-linear Poisson–Boltzmann theory, the characteristics of small ions dominate the properties of the electrical double layer of non-highly charged colloids, independently if the smallest ions are coions or counterions.[24]

Returning to the predominance of semi-punctual counterions at large electric fields, it is remarkable that its seeming "obviousness" was taken for granted, in general, in later electrical double layer investigations. In fact, this mean field recipe has led many researchers to unfoundedly extend its validity to the case of genuine hard-sphere ions of arbitrary size and valence close to a charged surface,[2,25–34] which corresponds to the so-called "unrestricted" primitive model of the electrical double layer. The direct application of the dominance principle, stated by Valleau and Torrie exclusively in the non-linear Poisson–Boltzmann framework,

to the primitive model of colloidal systems is neither appropriate nor justified when ion correlations and ionic excluded volume effects are relevant. On the other hand, some of the present authors have showed in a couple of previous papers[3,5] that, precisely, and contrary to the common belief, the counterions do not dominate or determine the properties of the primitive model electrical double layer. In these articles it was found that, at large colloidal charges, the behaviour of the primitive model electrical double layer associated with a *z:z* size-asymmetric electrolyte does not converge to that of a *z:z* size-symmetric electrolyte when the properties of counterions (such as the ionic size, valence, and concentration) are the same in both electrolytes. That is, it has been evinced in previous works that the characteristics of the coions in *z:z* electrolytes, symmetric in valence and asymmetric in size, are relevant and do matter for highly electrified colloids at high salt concentrations.

The aforementioned non-dominance of hard-sphere counterions has been clearly corroborated by theories and computer experiments[35–37] in recent studies. However, in all these articles this has been done exclusively for size-asymmetric primitive model systems. From that evidence, a working hypothesis that could transpire is that the origin of the non-dominance of counterions in the unrestricted primitive model resides solely in the ionic size-asymmetry. Thus, one of our main goals in this study is to show explicitly that the non-dominance of counterions is not restricted to occur only in the presence of unequally-sized electrolytes with symmetric *z:z* valences, but it can also arise in the presence of equally-sized electrolytes (*i.e.*, in the "plain" restricted primitive model of the electrical double layer) with asymmetric valences (monovalent counterions and multivalent coions). With this aim in mind, a reputed theoretical integral equation approach[1,38] and Monte Carlo computer simulations are used to analyze the electrostatic screening of a charged colloid under several conditions. Specifically, the behaviour of the mean electrostatic potential at the closest approach distance of ions to the colloidal surface, which is the so-called Helmholtz plane, is studied as a function of the colloidal surface charge density, the ionic volume fraction, and the valence of multivalent coions in the spherical and planar geometric instances of the colloidal particle. In addition to the non-dominance of counterions, an unexpected non-monotonic order, or precedence, in the electrostatic screening of the colloidal particle at the Helmholtz plane is observed. This interesting outcome is rationalized in terms of the spatial decay rate exhibited by the electric field near the colloidal surface, and by the appearance of a local inversion of both the electric field and the integrated surface charge density of the colloid, which is promoted by monovalent counterions and multivalent coions at high electrolyte concentrations.

2 Model system, simulations, and theories

Our representation of the electrical double layer is based on the well-known restricted primitive model of a binary electrolyte. In this description, a colloid is represented by a hard and

This journal is © the Owner Societies 2016

Phys. Chem. Chem. Phys., 2016, **18**, 21852–21864 | **21853**

uniformly charged sphere of radius R_M and surface charge density $\sigma_0 = Q_M/(4\pi R_M^2)$, where $Q_M = Z_M e$ is the colloidal charge, Z_M is the valence of the colloid, and e is the protonic charge. The spherical macroion is surrounded by an equally-sized z:1 electrolyte, asymmetric in valence, with monovalent counterions. Ions are represented by hard spheres of diameter a with point charges $q_i = z_i e$ embedded at their centers, such that z_i is the valence of the ionic species i. The spherical macroion and all ions are immersed in a continuum aqueous solvent characterized by a dielectric constant $\varepsilon = 78.5$ at a temperature $T = 298$ K in all instances.

The pair interaction potential between any pair of charged particles in spherical geometry, used in Monte Carlo simulations and integral equation theory, is given by:

$$U_{ij}(r) = \begin{cases} \infty, & r < r_i + r_j, \\ \dfrac{z_i z_j e^2}{4\pi\varepsilon_0\varepsilon r}, & r \geq r_i + r_j, \end{cases} \tag{1}$$

where the subscripts $i, j = M, +, -$; and r denotes the distance between the centers of two charged particles of types i and j with radii r_i and r_j, respectively.

As mentioned above, the closest approach distance between the ions of diameter a and the macroion of radius R_M is the so-called Helmholtz plane $r_H = R_M + (a/2)$, which is shown schematically in Fig. 1 (note our conventional use of the word "plane" instead of "surface"). The planar limit of the electrical double layer in our theory is obtained when both the valence and the radius of the macroion tend to infinity but the colloidal surface charge density remains constant. In this instance, the Helmholtz plane is located at an ionic radius $a/2$ from the colloidal surface.

Monte Carlo simulations of the electrical double layer in the presence of an infinite charged plate are performed in the canonical ensemble using a simulation box of volume $V = HL^2$, and cross section area $A = L^2$. Periodic boundary conditions along the y- and z-directions, and a finite length H along the x-axis are considered. The interaction between an ion i and an ion j is defined as the two-body interaction given by eqn (1). According to this definition, the hard-sphere interaction between

ions i and j, $S_{ij}(r)$, is zero if both particles do not overlap, and $S_{ij}(r) = \infty$ otherwise. The two-body electrostatic interaction between ions i and j is coulombic. The interaction between an ion i at the position $\vec{r}$ and the charged plate can also be separated into two contributions: a one-body hard-sphere interaction and a one-body electrostatic potential. The one-body hard-sphere interaction can be written as $S_i(x) = 0$, if the distance between the charged plate and the position of the ion i along the x-axis is such that $a/2 < x < H - (a/2)$, in other words, when there is no overlapping between the ion i and the two hard planes located at $x' = 0$ and $x' = H$. The hard plane located at $x' = 0$ has a surface charge density σ_0, and the hard plane located at $x' = H$ is neutral.

The one-body electrostatic energy between an ion i and the charged plate is given by

$$U_i^{\text{plate}}(x) = -\frac{\sigma_0 z_i e}{\varepsilon_0\varepsilon}|x|. \tag{2}$$

In summary, the one-body and two-body interactions can be written as

$$H_i^{\text{one-body}}(x) = S_i(x) + U_i^{\text{plate}}(x) \tag{3}$$

and

$$H_{ij}^{\text{two-body}}(r) = S_{ij}(r) + U_{ij}(r). \tag{4}$$

The total energy of the system is then defined as

$$H_T = \sum_{i=1}^{N} H_i^{\text{one-body}}(x) + \frac{1}{2}\sum_{i=1}^{N}\sum_{j=1}^{N} H_{ij}^{\text{two-body}}(r), \tag{5}$$

where $i \neq j$, and N is the total number of particles. Electrostatics are properly included via the Torrie and Valleau's charged-sheets method[39] using Boda's modification.[40]

Once the ionic profiles, $\rho_i(x)$, have been determined, it is possible to calculate the mean electrostatic potential as a function of the distance to the charged plate. If the reference mean electrostatic potential is zero in the bulk electrolyte located at $x = H/2$, we can define the integrated surface charge density as

$$\sigma(x) = \int_0^{h_x} \sum_i \rho_i(t) e z_i \, dt, \tag{6}$$

for $i = +, -$, with $h_x = (H/2) - x$, and $0 < x < (H/2)$. Applying the Gauss law, the electric field (perpendicular to the infinite charged plate) is given by

$$E(x) = \frac{\sigma(x)}{\varepsilon_0\varepsilon}. \tag{7}$$

The mean electrostatic potential as a function of the distance to the plate is then calculated from the electric field as

$$\Psi(x) = -\int_0^{h_x} E(t)\,dt = \int_{h_x}^0 E(t)\,dt. \tag{8}$$

The length of H in the simulations is chosen to be large enough to mimic a bulk electrolyte reservoir. We have monitored this condition, obtaining the desired bulk electrolyte concentration with an error of less than 1%. The total number of particles in the simulation box varied from 2000 for salts with trivalent coions up to 5000 for electrolytes with monovalent coions.
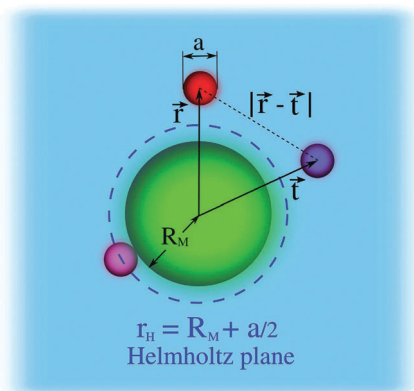

Fig. 1   Schematic representation of the model system.

21854 | Phys. Chem. Chem. Phys., 2016, 18, 21852–21864

This journal is © the Owner Societies 2016

In all instances, 5×10^4 Monte Carlo cycles were performed to equilibrate the system. The canonical average was calculated using 3×10^5 Monte Carlo cycles for high colloidal charges and 9×10^5 Monte Carlo cycles for low colloidal charges.

On the other hand, Monte Carlo simulations of the spherical electrical double layer are performed in a cubic simulation box in the canonical ensemble under periodic boundary conditions. The spherical charged colloid is placed in the center of the simulation box and is not allowed to move. Ewald sums with conducting boundary conditions are used to take into account correctly the long-range behaviour of Coulomb interactions. The damping constant is $\alpha = 5/L$, with L the length of the cubic simulation box. 725 vectors in the k-space are used to compute the reciprocal space contribution to the Coulomb energy. If we denote N_+ and N_- as the number of cations and anions in the simulation box, respectively, the electroneutrality condition imposed in our simulations is given by $Z_M + N_+ z_+ + N_- z_- = 0$. The number of particles employed in each run for the spherical geometry has been around 3500. For the equilibration process 1×10^5 Monte Carlo cycles have been performed. 4×10^5 and 10×10^5 Monte Carlo cycles have been carried out to calculate the canonical average of systems with high and low colloidal charges, respectively.

Complementarily, the integral equation description is obtained by solving numerically the Ornstein–Zernike equations using the hypernetted-chain/mean spherical approximation (HNC/MSA) closure. The Ornstein–Zernike equations describing the ionic cloud around a single macroion can be written as

$$h_{Mj}(r) = c_{Mj}(r) + \sum_{k=-,+} \rho_k \int h_{Mk}(t) c_{kj}\left(|\vec{r} - \vec{t}|\right) \mathrm{d}V, \quad \text{for } j = -, +, \tag{9}$$

where $h_{Mj}(r) = g_{Mj}(r) - 1$ are the total ionic correlation functions, and $g_{Mj}(r)$ are the ionic radial distribution functions. The direct correlation functions between ions and the spherical colloid are specified using the hypernetted-chain (HNC) closure $c_{Mj}(r) = -\beta U_{Mj}(r) + h_{Mj}(r) - \ln[h_{Mj}(r) + 1]$. Ion–ion direct correlation functions $c_{kj}(|\vec{r} - \vec{t}|)$ are approximated by the analytical mean spherical approximation (MSA) expressions for a bulk electrolyte at a concentration ρ_k.[41,42] These equations are a complete set of integral equations that are solved numerically *via* an efficient finite element method.[38] If $c_{kj}(|\vec{r} - \vec{t}|) = -(z_k z_j e^2)/(4\pi\varepsilon_0\varepsilon|\vec{r} - \vec{t}|)$ is used instead of the interionic MSA direct correlation functions in eqn (9), the integral equation version of the non-linear Poisson–Boltzmann theory is obtained. In this last mean field approach, ion correlations and excluded volume effects are neglected in the description of the diffuse ionic cloud. In both approaches, *i.e.*, the HNC/MSA integral equation theory and the non-linear Poisson–Boltzmann formalism, the planar limit can be obtained numerically by using a macroion with a diameter of 6000 Å. We have estimated that the error between the ionic profiles in the planar geometry and around a spherical colloid with a diameter of 6000 Å is less than 1% in both theoretical approaches (HNC/MSA integral equations and the non-linear Poisson–Boltzmann) by calculating the limit of the counterions' contact value when the diameter of the colloid goes to infinity.

From the ionic profiles obtained from simulations or theory in spherical geometry, it is possible to calculate several thermodynamic and electrical properties of the charged particles in solution. Specifically, the integrated charge, the electric field, and the mean electrostatic potential around a spherical macroion can be written, respectively, as

$$P(r) = z_M + \sum_{i=-,+} \int_0^r z_i \rho_i g_i(t) 4\pi t^2 \mathrm{d}t, \tag{10}$$

$$E(r) = \frac{e}{4\pi\varepsilon_0\varepsilon} \frac{P(r)}{r^2}, \tag{11}$$

and

$$\Psi(r) = -\int_\infty^r E(t)\mathrm{d}t = \int_r^\infty E(t)\mathrm{d}t. \tag{12}$$

Physically, the integrated charge is the net charge (in units of e) enclosed in a sphere of radius r centered in the macroion, and is a measure of the neutralization capacity of the surrounding electrolyte. The electric field is proportional to the electrostatic component of the mean force that a charged particle experience due to its coulombic interaction with the colloidal particle and the ions of the electrolyte. The mean electrostatic potential quantifies the electrostatic screening of the bare colloidal charge by the electrolyte. The mean electrostatic potential evaluated close to the Helmholtz plane has been conventionally associated with the so-called zeta potential, ζ. This last quantity is usually defined as the mean electrostatic potential at the slipping plane in electrokinetic phenomena.

3 Results and discussion

In order to introduce the concept of the non-dominance of counterions, and as a contrast, we would like to exemplify first the opposite phenomenon, that is, the dominance of counterions according to the non-linear Poisson–Boltzmann theory in spherical geometry. With this goal in mind, let us consider a spherical macroion of radius $R_M = 15$ Å in the presence of several z:1 semi-punctual electrolytes with a unique ionic closest approach distance $a/2 = 2.125$ Å regarding the surface of the macroion. As mentioned in the Introduction, ions have a dual behaviour in our version of the non-linear Poisson–Boltzmann theory: they interact among them as point particles but they also have an ionic size associated with their interaction with the charged colloid. The closest approach distance between the ions and the spherical colloid, or the Helmholtz plane, is located at a distance $R_M + (a/2)$ (see Fig. 1). Note that the current description corresponds to the Stern model in the absence of specific ionic adsorption in the region located between the colloidal surface and the onset of the ionic diffuse layer at the Helmholtz plane. Here and hereinafter, the colloidal surface charge density is positive and the concentration of the monovalent anions (counterions) in the z:1 electrolytes is always 1 M, in order to have electrolytes whose anions (counterions) have the same properties in both the spherical and planar limits for a given ionic size. The concentration of multivalent z cations (coions) is
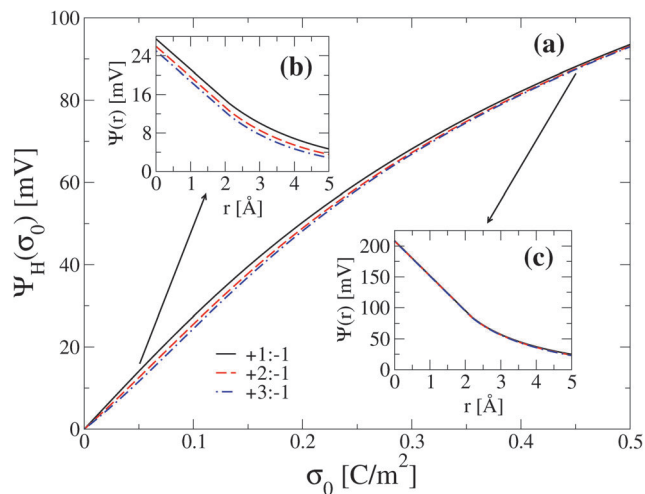
Fig. 2 The dominance of counterions in non-linear Poisson–Boltzmann theory for spherical geometry. In all panels the radius of the macroion is 15 Å, and the closest approach distance between the colloidal surface and the semi-punctual cations and anions is 2.125 Å. The mean electrostatic potential is plotted for several z:1 electrolytes as follows: (a) at the Helmholtz plane as a function of the surface charge density of the macroion, (b) as a function of the distance to the surface of the macroion for a surface charge density $\sigma_0 = 0.05$ C m^{-2}, and (c) as a function of the distance to the surface of the macroion for a surface charge density $\sigma_0 = 0.45$ C m^{-2}. In this figure and hereinafter, the concentration of the monovalent anions is 1 M and the concentration of multivalent cations is such that the electroneutrality condition is fulfilled.

adjusted to satisfy the electroneutrality condition of the whole system. The mean electrostatic potential at the Helmholtz plane, according to the non-linear Poisson–Boltzmann theory, is then shown in Fig. 2(a) as a function of the colloidal surface charge density σ_0 in the presence of different z:1 electrolytes. Here, we observe that the value of the mean electrostatic potential at the Helmholtz plane converges to the same curve for all the different z:1 electrolytes in the limit of large colloidal charges. Such a convergence occurs not only at the Helmholtz plane but at all distances from the colloidal surface as shown in Fig. 2(c), indicating that the corresponding ionic density profiles (not shown) also converge to the same limit. At low colloidal charges, the mean electrostatic potential is clearly different for each z:1 electrolyte as shown in Fig. 2(b). Thus, the convergence of the ionic density profiles and mean electrostatic potential in the presence of z:1 semi-punctual electrolytes at large colloidal charges illustrates the dominance of counterions in the electrical double layer of equally-sized electrolytes asymmetric in valence. Such a dominance of counterions is analogous to that shown by Valleau and Torrie in 1982 using a size-asymmetric electrolyte, symmetric in valence, near an infinite planar electrode.[23] An important consequence of the dominance of counterions predicted by the non-linear Poisson–Boltzmann theory is that the properties of coions (such as their ionic "size", valence, or concentration) are certainly irrelevant in the limit of strong electric fields according to this mean field picture.

Two ingredients that are missing in the classical Poisson–Boltzmann description are ion correlations and ionic excluded

volume effects. Physically, the former include the preference of ions to be surrounded by ions of opposite charge and not by ions of the same sign, whereas the latter takes into account the fact that hydrated finite-sized ions cannot overlap as occurs in the case of point charges. The result of including ion correlations and ionic excluded volume effects in the description of the spherical electrical double layer is now displayed in Fig. 3(a) using theory and simulation. Here, the mean electrostatic potential at the Helmholtz plane around a spherical macroion of radius $R_M = 15$ Å is displayed for several z:1 equally-sized primitive model electrolytes with radius $a/2 = 2.125$ Å. At low surface charge densities of the spherical macroion, the Monte Carlo simulations and integral equation data of Fig. 3(a) show that the maximum electrostatic screening (or minimum potential) at the Helmholtz plane is produced by the electrolyte whose coions have the largest valence z. An analogous behaviour has been already observed in the non-linear Poisson–Boltzmann picture (see, *e.g.*, Fig. 2(a)). Note, however, that such a trend observed in Fig. 3(a) is inverted at high surface charge densities of the macroion according to simulations and integral equation theory. In addition, the continuous theoretical curves display a surface charge density of the macroion, σ_0', with the property that the mean electrostatic potential at the Helmholtz plane has approximately the same value for all equally-sized z:1 electrolytes, asymmetric in valence. At surface charge densities of the macroion lower than σ_0' it is observed that electrolytes with multivalent coions screen more effectively the bare colloidal charge of the macroion at the Helmholtz plane, that is, $\Psi(r = R_M + (a/2), \sigma_0, z_A) < \Psi(r = R_M + (a/2), \sigma_0, z_B)$ if $\sigma_0 < \sigma_0'$ and $z_A > z_B$, where z_A and z_B are the valences of coions of electrolytes A and B, respectively. Under these conditions, a particular order or precedence in the electrostatic screening at the Helmholtz plane as a function of the coion's valence can be observed. Contrastingly, if the colloidal surface charge density of the macroion is larger than σ_0' then the opposite behaviour is observed: in this case the mean electrostatic potential at the Helmholtz plane is screened less effectively when the valence of coions augments, that is, $\Psi(r = R_M + (a/2), \sigma_0, z_A) < \Psi(r = R_M + (a/2), \sigma_0, z_B)$ if $\sigma_0 > \sigma_0'$ and $z_A < z_B$. Thus, the observed order or precedence in the electrostatic screening at the Helmholtz plane as a function of the coion's valence is inverted depending on the specific value of the bare colloidal charge. On the other side, simulation and theoretical data evidence that the maximum difference in the mean electrostatic potential at the Helmholtz plane among equally-sized z:1 electrolytes, asymmetric in valence, occurs at very high surface charge densities of the colloid. This behaviour confirms precisely one of our main theses, namely that the non-dominance of counterions can also be promoted by an asymmetry in the valence of equally-sized electrolytes and constitutes an outstanding result of this study. In other words, we are explicitly demonstrating here that, in addition to the mechanism of the ionic-size asymmetry of z:z electrolytes, symmetric in valence,[3,5] the breaking of the symmetry in the valence of z:1 equally-sized electrolytes is sufficient to produce qualitative differences in the properties of the electrical double layer of highly charged macroions when the monovalent
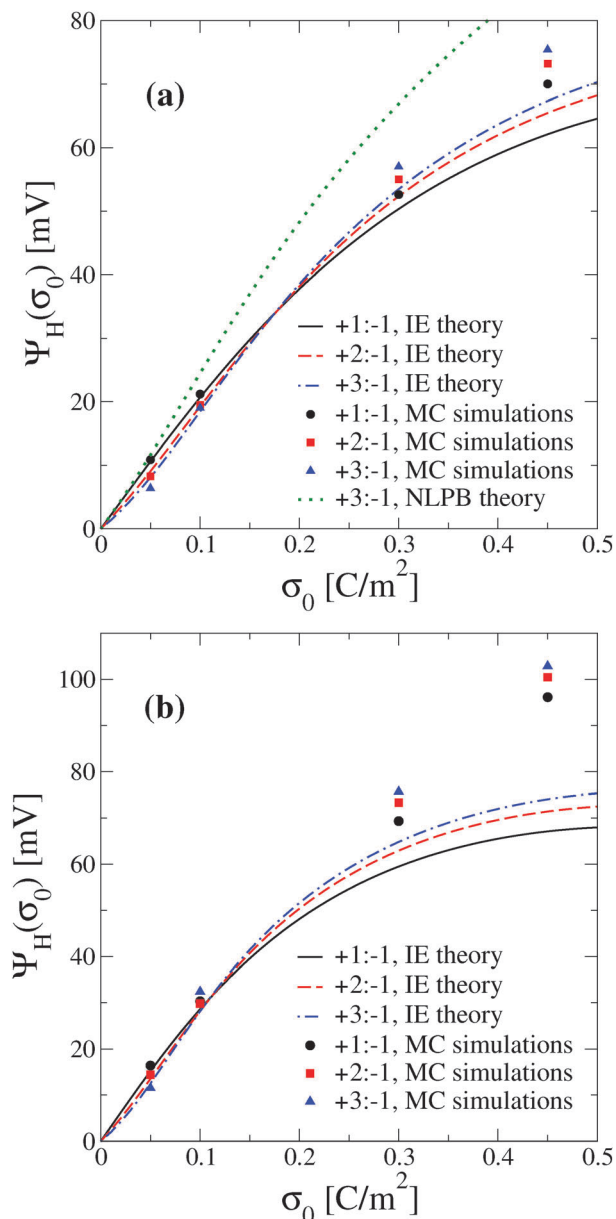
Fig. 3 Mean electrostatic potential at the Helmholtz plane as a function of the surface charge density, σ_0, of a macroion for several $z{:}1$ electrolytes. In all instances, the radius of cations and anions is 2.125 Å. In the integral equation theory (IE), the radius of the colloid is 15 Å and 3000 Å in panels (a) and (b), respectively. In the Monte Carlo simulations (MC), the radius of the colloid is 15 Å in panel (a), and the colloid is an infinite planar electrode in panel (b). Solid symbols and lines correspond to Monte Carlo simulations and integral equation results, respectively. The mean electrostatic potential in the presence of a $+3{:}-1$ electrolyte displayed in Fig. 2 for non-linear Poisson–Boltzmann (NLPB) theory has been included in panel (a) as a dotted line for comparison purposes.

counterions have the same properties in all instances and coions are multivalent. Given that ion correlations and ionic excluded volume effects are not included in the Poisson–Boltzmann theory, the non-dominance of counterions appears as a consequence of these ingredients, which represents a new insight into the theory of the electrical double layer.

In order to analyze the role of the macroion's size in the non-dominance of counterions when equisized electrolytes asymmetric in valence are present, the mean electrostatic potential produced by an infinite planar electrode at the Helmholtz plane is shown in Fig. 3(b) for the same electrolytes displayed in Fig. 3(a). In this case, it is observed that the magnitude of the mean electrostatic potential in planar geometry is larger regarding the spherical geometry, which is physically due to the augmentation in the strength of the electric field for the same surface charge density. Simulation and theoretical results display similar features to those already observed in Fig. 3(a), that is, (i) the non-dominance of counterions at large surface charge densities; (ii) the existence of a surface charge density σ_0' whose magnitude determines the efficiency of equally-sized $z{:}1$ electrolytes, asymmetric in valence, to screen electrostatically the bare surface charge of the electrode at the Helmholtz plane; and (iii) a non-monotonic order or precedence in the magnitude of the mean electrostatic potential (or screening) at the Helmholtz plane associated with electrolytes that only differ in the valence and concentration of multivalent coions. One important difference between Fig. 3(a) and (b) is that the magnitude of σ_0' is lower for the infinite planar electrode in comparison with the spherical macroion. As a result, the inversion of the ordering or precedence of the electrostatic potential at the Helmholtz plane for electrolytes with multivalent coions can be observed at lower surface charge densities in planar geometry with respect to the spherical geometry.

With the aim of evaluating the role of the ionic volume fraction associated with a given ionic size (due, *e.g.*, to a different degree of hydration) in the non-dominance of counterions, we study now the electrical double layer of a spherical macroion of radius $R_M = 15$ Å immersed in several equally-sized $z{:}1$ electrolytes, asymmetric in valence, with an ionic radius of $a/2 = 3.3$ Å. The mean electrostatic potential at the Helmholtz plane obtained *via* simulations and integral equation theory as a function of σ_0 is portrayed in Fig. 4(a). Here, a behaviour similar to that displayed in Fig. 3(a) is observed, *i.e.*, (i) the mean electrostatic potential at the Helmholtz plane is different among several equally-sized $z{:}1$ electrolytes surrounding a highly charged macroion when the properties of counterions are the same; (ii) there is a surface charge density σ_0' for which the mean electrostatic potential is approximately the same; and (iii) the order or precedence of the electrostatic screening of the colloidal charge at the Helmholtz plane is not monotonic but inverts. On the other hand, some noticeable differences between Fig. 3(a) and 4(a) are that (i) the magnitude of σ_0' decreases when the ionic volume fraction increases and (ii) the global curvature of the mean electrostatic potential in Fig. 4(a) is inverted regarding the curvarture displayed in Fig. 3(a).

The effect of increasing the size of the macroion and the ionic volume fraction simultaneously is analyzed in Fig. 4(b). Here, the mean electrostatic potential at the Helmholtz plane is plotted for different $z{:}1$ equally-sized electrolytes next to an infinite charged plate of varying σ_0. The ionic radius of all electrolytes is $a/2 = 3.3$ Å. In this instance, simulation and theoretical results also confirm the non-dominance of counterions at large
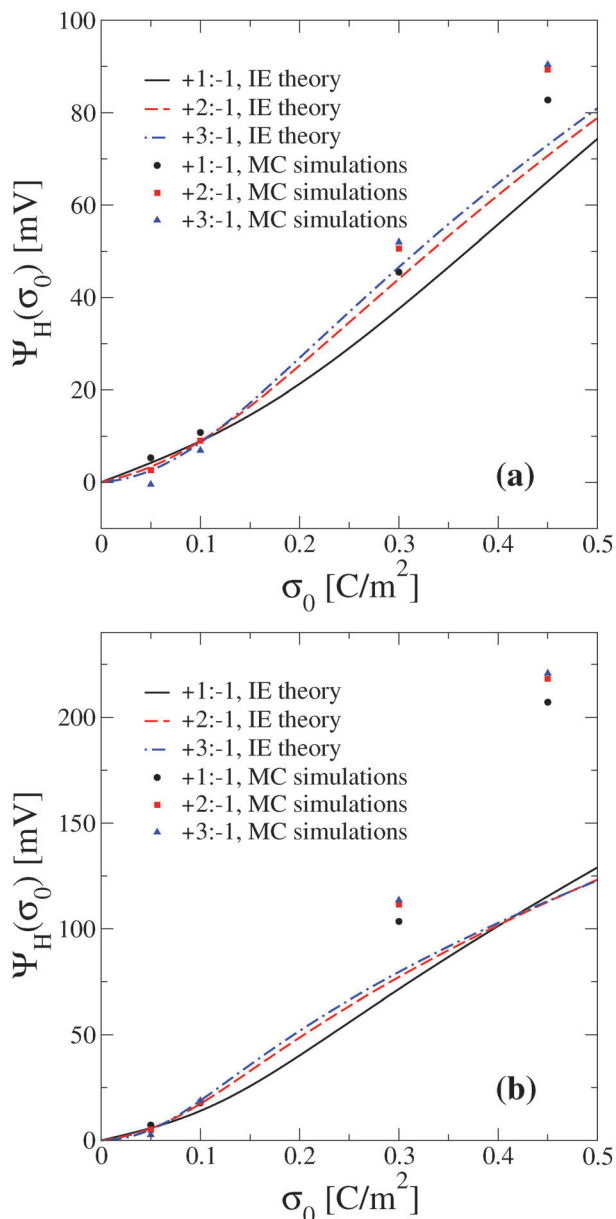
This journal is © the Owner Societies 2016

Phys. Chem. Chem. Phys., 2016, **18**, 21852–21864 | 21857

Fig. 4 Mean electrostatic potential at the Helmholtz plane as a function of the surface charge density, σ_0, of a macroion for several z:1 electrolytes. In all instances, the radius of cations and anions is 3.3 Å. Panels (a) and (b) correspond to the spherical and planar geometries, respectively, as described in Fig. 3. Symbols and lines in both panels follow the same conventions defined in Fig. 3.

electric fields. Even though the electrostatic potential seems to converge for electrolytes 1:2 and 1:3 according to integral equation theory data, these curves actually diverge at larger colloidal charges (not shown). In addition, Monte Carlo simulations and integral equation theory show that augmentation of the ionic volume fraction is able to reduce the magnitude of the surface charge density σ_0' at which the order or precedence in the electrostatic screening at the Helmholtz plane inverts.

We now proceed to discuss in more fundamental terms the non-dominance of counterions and the order or precedence in the mean electrostatic potential, which can be rationalized in terms of the associated electric field. According to eqn (8) and (12), the mean electrostatic potential at the Helmholtz plane is an integral, or functional, of the spatial electric field in planar and spherical geometries. In the planar instance, the electric field is stronger regarding the spherical geometry for the same surface charge density and, accordingly, the electrostatic effects are more conspicuous. Another advantageous feature of the planar geometry is that, in this instance, the electric field is directly proportional to the integrated surface charge density (see, *e.g.*, eqn (7)), which is a measure of the neutralization capacity of the bathing electrolyte. Thus, now we analyze our Monte Carlo simulations of the electric field in the planar limit as a function of the ionic size (or the ionic volume fraction), the valence of coions, and the charge of the electrode. The electric field surrounding an infinite planar electrode immersed in different size-symmetric z:1 electrolytes asymmetric in valence is displayed in Fig. 5 for two different surface charge densities. In both instances, the ionic radius of cations and anions is $a/2 = 2.125$ Å. The electric field associated with a surface charge density $\sigma_0 = 0.05$ C m^{-2} of the electrode is plotted in Fig. 5(a). In this figure, we observe that the electric field as a function of the distance to the electrode's surface is overall lower for electrolytes with larger coion's valences, that is, $E(x,z_A) < E(x,z_B)$ if $z_A > z_B$. Here and hereinafter, z_A and z_B denote the valences of coions of cases A and B, respectively. More importantly, we observe that the sign of the electric field inverts locally even in the presence of monovalent counterions if multivalent coions are present. In the past, a local inversion of the electric field around a charged colloid has been associated with the phenomena of charge inversion and local charge reversal.[43–45] Charge inversion is the interchange of roles between counterions and coions at some distance from the electrified surface, whereas local charge reversal is the local over-compensation of the bare colloidal charge by counterions.[43] Such phenomena have been observed experimentally, *e.g.*, in aqueous dispersions of charged colloids with strong electrostatic correlations due to the presence of multivalent counterions.[46–49] Then, to our best knowledge, this is the first time in which a local inversion of both the electric field and the integrated charge of a colloid is predicted in aqueous primitive model electrolytes containing solely monovalent counterions and multivalent coions. As a result, a new insight into the occurrence of charge inversion and local charge reversal in the absence of multivalent counterions and specific ionic short-range attractions is provided. On the other hand, note that the magnitude of the inverted electric field increases as a function of the coion's valence as is shown in the inset of Fig. 5(a). This effect and the faster decay of the electric field near the electrode's surface for coions with a larger valence explains the order or precedence displayed by the mean electrostatic potential at the Helmholtz plane in Fig. 3(b) for low/moderate colloidal surface charge densities.

The electric field as a function of the distance to the surface of the charged electrode is shown in Fig. 5(b) under the same conditions used in Fig. 5(a), except that this time the surface charge density has a value $\sigma_0 = 0.3$ C m^{-2}. In this instance, we observe that the decay of the electric field near the electrode's surface displays the opposite behaviour previously observed at
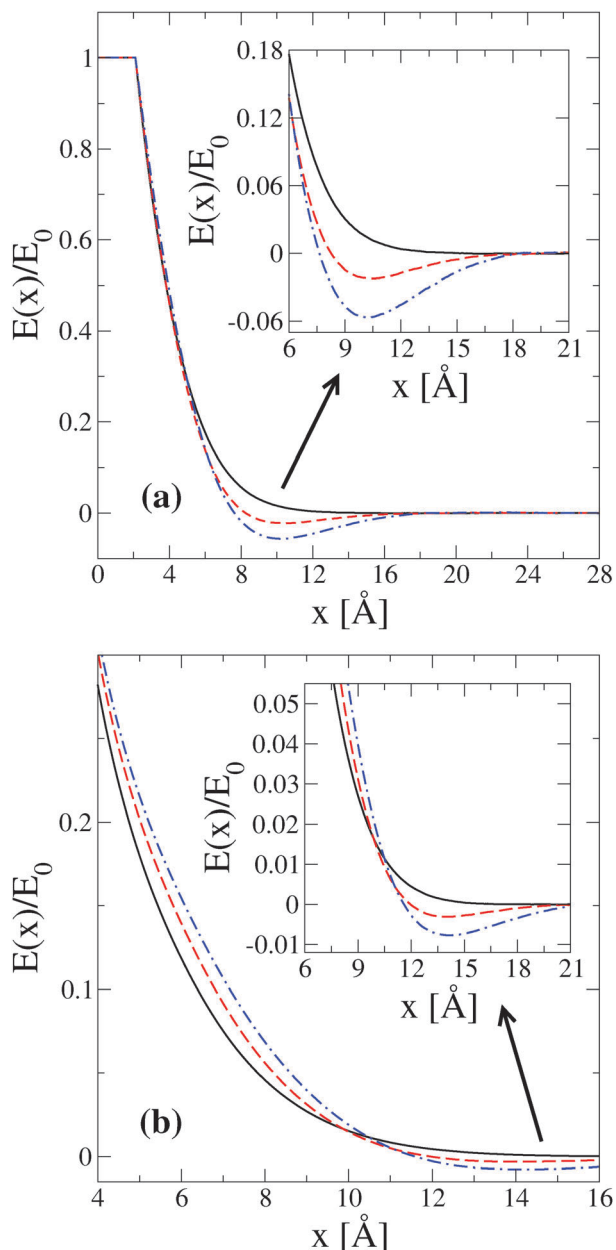
Paper

Fig. 5 Monte Carlo simulations of the electric field as a function of the distance to the surface of an infinite charged planar electrode for several z:1 electrolytes. Solid, dashed, and dotted-dashed lines correspond to coions with valences $z = 1$, 2, and 3, respectively. $E_0 = \sigma_0/(\varepsilon_0\varepsilon)$ denotes the electric field at the surface of the charged electrode located at $x = 0$. The surface charge density, σ_0, of the electrode is 0.05 C m^{-2} in panel (a) and 0.3 C m^{-2} in panel (b). Insets display magnifications for comparison purposes. In all instances, the radius of cations and anions is 2.125 Å.

the lower surface charge density $\sigma_0 = 0.05$ C m^{-2}. This time, the electric field is lower for electrolytes with smaller coion's valences, that is $E(x,z_A) < E(x,z_B)$ if $z_A < z_B$ and $x < x'$, where $x' \approx 10.5$ Å. Here and hereinafter, x' and x'' are distances from the electrode's surface where the electric field is approximately the same for all electrolytes and $x' < x''$. In Fig. 5(b), it is observed that the local inversion of the electric field previously observed in Fig. 5(a) is still present when the surface charge

density increases. However, the location of the maximum inversion of the electric field is shifted to the right (far away from the electrode's surface). More importantly, the magnitude of the maximum inversion of the electric field in this case is significantly lower regarding the magnitude of the maximum inversion of the electric field previously observed at a lower surface charge density (compare, *e.g.*, the insets of Fig. 5(a) and (b)). As a result, the contribution of the electric field in the region $x > x'$ to the integral, or functional, that defines the mean electrostatic potential at the Helmholtz plane (see, *e.g.*, eqn (8)) is smaller with regard to the contribution of the electric field in the region $x < x'$. Thus, the decay of the electric field close to the electrode's surface as a function of the coion's valence in Fig. 5(b) mainly determines the order or precedence in the mean electrostatic potential at the Helmholtz plane displayed in Fig. 3(b) for high colloidal surface charge densities.

The effect of increasing the ionic volume fraction on the behaviour of the electric field is studied in Fig. 6. In Fig. 6(a), the electric field as a function of the distance to the electrode's surface is displayed under the same conditions used in Fig. 5(a), except that the ionic radius of cations and anions is $a/2 = 3.3$ Å. In this case, we notice again that the electric field is overall lower for electrolytes with larger coion's valence close to the electrode's surface, that is $E(x,z_A) < E(x,z_B)$ if $z_A > z_B$ and $x < x'$, where $x' \approx 15$ Å. The location of the maximum inversion of the electric field (around 10 Å) is approximately the same for the ionic volume fractions used in Fig. 5 and 6, which correspond to electrolytes with ionic radius $a/2 = 2.125$ Å and $a/2 = 3.3$ Å, respectively. Notice, however, that the magnitude of the maximum inversion of the electric field is significantly larger for the electrolytes with the largest ionic size or highest ionic volume fraction. In the case of trivalent coions, we observe that the magnitude of the maximum inversion of the electric field can be as large as one quarter of the electric field at the electrode's surface (see, *e.g.*, the inset of Fig. 6(a)). The order or precedence of the electric field observed for $x < x'$ is now inverted in the region $x' < x < x''$, that is this time $E(x,z_A) < E(x,z_B)$, if $z_A < z_B$, where $x'' \approx 25$ Å. The electric field displays a maximum in the region $x' < x < x''$, whose magnitude is, however, significantly smaller regarding the magnitude of the maximum inversion of the electric field observed for $x < x'$. Additional inversions in the order or precedence of the electric field are observed for $x > x''$. Notwithstanding, their maximum magnitudes are very small and decrease very rapidly far away from the electrode's surface. The contribution of the electric field in the region $x > x'$ to the functional, or integral, corresponding to the mean electrostatic potential at the Helmholtz plane (see, *e.g.*, eqn (8)) is then significantly smaller than the contribution of the electric field in the region $x < x'$. As a result, the order or precedence displayed by the electric field as a function of the coion's valence in the region $x < x'$ mainly determines the behaviour of the mean electrostatic potential curves displayed in Fig. 4(b) for low colloidal surface charge densities.

In Fig. 6(b), the electric field as a function of the distance to the electrode's surface is displayed under the same conditions used in Fig. 6(a), except that the surface charge density of the

This journal is © the Owner Societies 2016

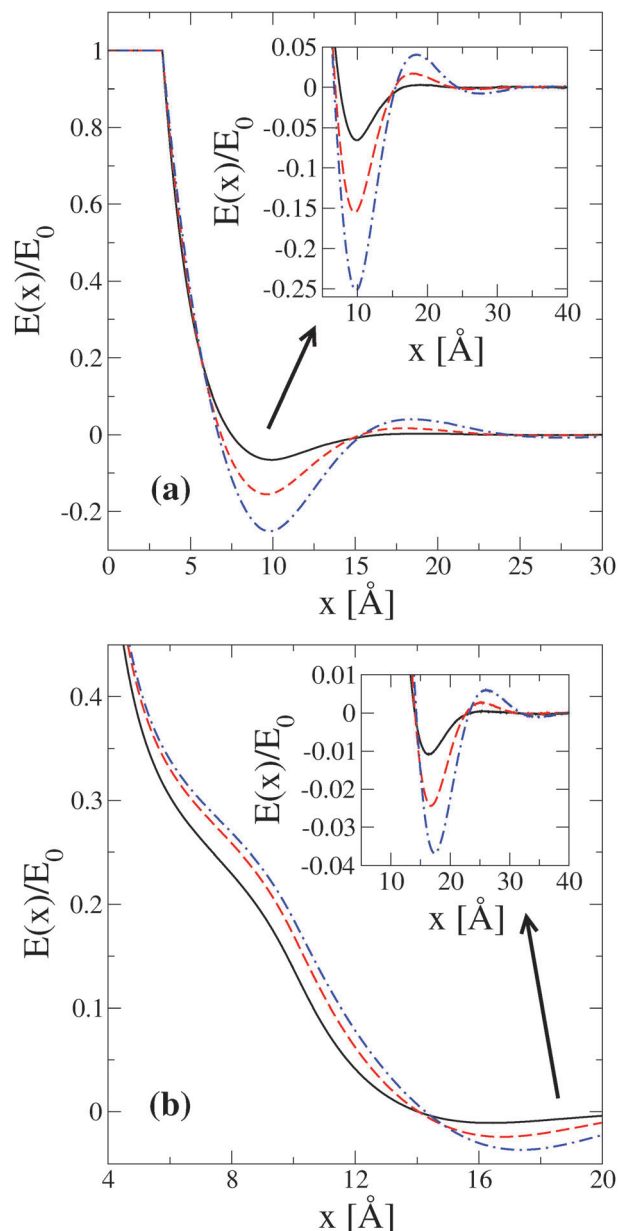*Phys. Chem. Chem. Phys.*, 2016, **18**, 21852–21864 | **21859**

Fig. 6 Monte Carlo simulations of the electric field as a function of the distance to the surface of an infinite charged planar electrode for several z:1 electrolytes. Solid, dashed, and dotted-dashed lines correspond to coions with valences z = 1, 2, and 3, respectively. $E_0 = \sigma_0/(\varepsilon_0 \varepsilon)$ denotes the electric field at the surface of the charged electrode located at $x = 0$. The surface charge density, σ_0, of the electrode is 0.05 C m^{-2} in panel (a) and 0.3 C m^{-2} in panel (b). Insets display magnifications for comparison purposes. The radius of cations and anions is 3.3 Å in all cases.

electrode is now $\sigma_0 = 0.3$ C m^{-2}. In this case, we observe that the decay of the electric field near the electrode's surface displays the opposite behaviour previously observed at the lower surface charge density $\sigma_0 = 0.05$ C m^{-2}, that is in this instance $E(x,z_A) < E(x,z_B)$ if $z_A < z_B$ and $x < x'$, where $x' \approx 14.5$ Å. For $x > x'$, we observe consecutive inversions in the order or precedence of the electric field. Again, the maximum local absolute values of the oscillating electric field decrease very rapidly far away from the electrode's surface. As the contribution of the electric

field in the region $x > x'$ to the integral, or functional, defining the mean electrostatic potential at the Helmholtz plane is smaller than the contribution of the electric field in the region $x < x'$, the order or precedence displayed by the electric field as a function of the coion's valence in the region $x < x'$ determines the order or precedence in the electrostatic screening displayed in Fig. 4(b) at moderate/high colloidal surface charge densities.

In order to gain further physical insight into the local inversion of the electric field in the presence of monovalent counterions and multivalent coions, in Fig. 7 we plot the simulation and theoretical ionic distribution functions (or reduced densities) associated with the electric field curves displayed in Fig. 6(a). In Fig. 7(a), Monte Carlo simulations show that anions (counterions) are significantly more adsorbed than cations (coions) at the surface of the positive planar electrode. The ionic concentrations of anions and cations follow the previous behaviour in a spatial region close to the surface of the planar electrode ($x < 10$ Å). However, in the region located between 10 and 17.5 Å it is observed that the previous precedence in the ionic concentration of anions and cations is slightly inverted, that is in this zone the ionic concentration of coions is slightly larger than the concentration of counterions. The inversion of roles of counterions and coions is precisely the so-called phenomenon of charge inversion, which is mainly promoted in this instance by ion correlations and ionic excluded volume effects associated with 1:1 hydrated electrolytes at large ionic volume fractions. Since the classical Poisson–Boltzmann description neglects these effects, the phenomenon of charge inversion is absent in such a description of semi-punctual ions. The effects of increasing the valence of coions, when the surface charge density of the electrode and the properties of the monovalent counterions are fixed, are illustrated in Fig. 7(b). Here, Monte Carlo simulations display that the ionic concentrations of cations and anions very near the colloidal surface are notably lower in the presence of divalent coions regarding the instance in which coions are monovalent (compare this figure with Fig. 7(a)). The phenomenon of charge inversion is also more conspicuous, and now it is possible to observe clearly the formation of a layer of divalent coions whose maximum is located around 12 Å approximately. The effects of further increasing the valence of coions is exemplified in Fig. 7(c). In this case, Monte Carlo simulations display that trivalent coions promote a larger depletion of the binary electrolyte very close to the colloidal surface with respect to the instance in which coions are monovalent or divalent (compare this figure with Fig. 7(a) and (b)). The height of the layer of coions is larger and its maximum is shifted far away from the colloidal surface (at around 12.6 Å approximately). Another interesting feature for trivalent coions is the appearance of an additional charge inversion, which is consistent with the small local oscillations in the electric field displayed in Fig. 6(a) far away from the colloidal surface. In addition, integral equation theory displays a good overall agreement regarding the Monte Carlo simulation data. The best quantitative agreement is observed in the presence of the 1:1 electrolyte. In this instance, it is observed that HNC/MSA overestimates the contact values of both ionic profiles, which is
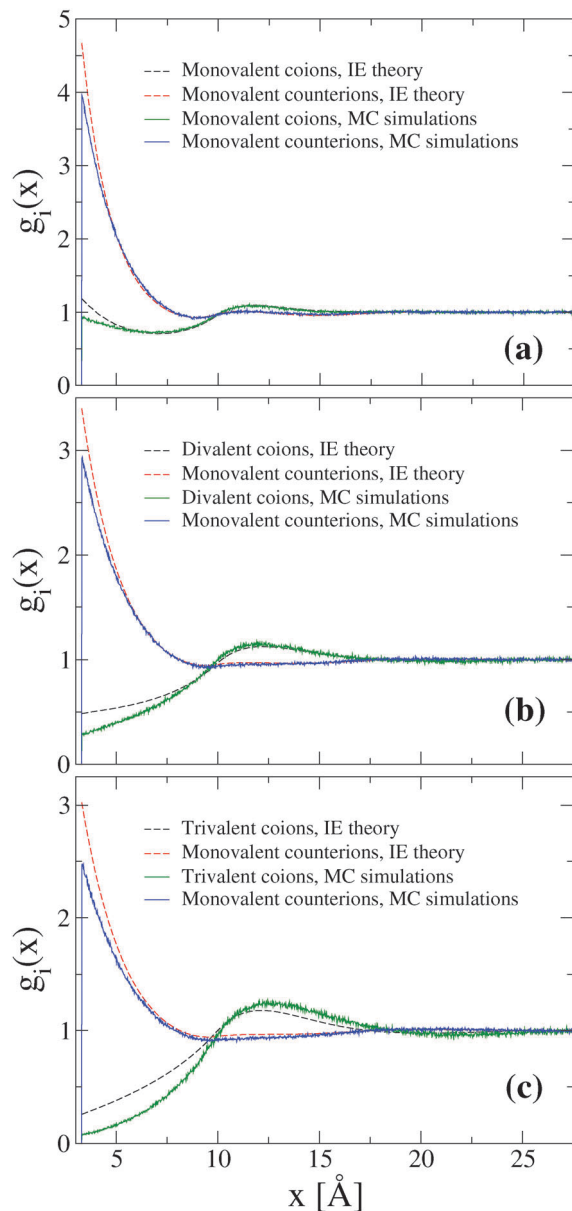
Fig. 7 Reduced ionic densities as a function of the distance to the surface of an infinite charged planar electrode for several z:1 electrolytes. In all instances, the surface charge density, σ_0, of the electrode is 0.05 C m^{-2}, the concentration of monovalent counterions (anions) is 1 M, and the radius of cations and anions is 3.3 Å. Panels (a)–(c) correspond to electrolytes whose coions (cations) have valences $z = 1$, 2, and 3, respectively. In the integral equation theory (IE), a spherical colloid of radius 3000 Å is used to represent theoretically a charged plane. In the Monte Carlo simulations (MC) the colloidal particle is an infinite charged planar electrode. Solid and dashed lines correspond to Monte Carlo simulations and integral equation results, respectively.

a well-known limitation of the HNC closure. When the valence of coions increases, the contact values of the binary electrolyte are further overestimated. Interestingly, the maximum height of the layer of multivalent coions and its location are approximately well described by the integral equation theory.

An experimental realization of the phenomenology discussed above is very appealing. In this regard, there are metallic oxide particles that are able to reach positive and negative surface charge densities as large as 0.6 C m^{-2} under appropriate pH conditions.[50,51] These extremely high colloidal charges correspond, in principle, to the physical limit where the non-dominance of counterions should be experimentally observed. Note, however, that our theoretical calculations and computer simulations suggest more modest surface charge densities, of the order of or less than 0.05 C m^{-2}, at which the phenomena of charge inversion, local charge reversal, and a local inversion of the electric field should be observed experimentally when they are promoted by multivalent coions and monovalent counterions in concentrated electrolytes. In fact, latex and silica particles with surface charge densities in this regime have been used in the past in several electrophoretic mobility experiments involving multivalent electrolytes.[48,52,53] On the other hand, surface charge densities larger than 0.2 C m^{-2} are required, in principle, to observe experimentally the non-dominance of counterions and an inversion in the order or precedence of the mean electrostatic potential at the Helmholtz plane near the colloid. Regarding the selection of electrolytes, ions usually do not have exactly the same ionic size in nature. In order to overcome this problem in the validation of our theoretical and simulation predictions, the same monovalent counterion should be chosen in all instances. Then, indifferent coions with approximately the same ionic size can be selected even if there is a slight size asymmetry regarding the ionic size of the monovalent counterion. The main idea is to have electrolytes that are almost identical and only differ in the valence and concentration of coions when the electroneutrality condition is fulfilled. For cationic colloids, Cl$^-$, NO$_3^-$, and ClO$_4^-$ anions could be used as counterions. As Na$^+$, Ca^{2+}, La^{3+}, and Th^{4+} cations have approximately the same ionic size,[54] they could be used as coions in the presence of positive colloidal particles. For anionic colloids, Na$^+$ cations could be used as counterions. Mono-, di-, and tri-basic phosphate anions (H$_2$PO$_4^-$, HPO$_4^{-2}$, and PO$_4^{-3}$) also have approximately the same ionic size and could be used as coions in the presence of negative colloidal particles. In fact, the electrophoretic mobility of iron oxide particles has been recently measured as a function of Na$^+$:z electrolytes, in which several mono- and divalent anions taken from the representative Hofmeister series were used.[55] Moreover, the disjoining pressure of foam films stabilized by an anionic surfactant in the presence of NaCl, Na$_2$SO$_4$, and Na$_3$ citrate has also been measured.[56] The results reported therein confirm that the ionic correlation effects are really significant in the cases of divalent and trivalent coions. The effect of multivalent coions on the electrical double layer of charged colloids has also been addressed in other experimental works.[57–59] In those studies, it has been shown that the valence of multivalent coions has a profound influence on the shape of the force curves between colloidal charged particles, and it has been proposed that the aggregation of equally charged particles in the presence of multivalent coions can be described by an inverse Schulze–Hardy rule. On the other hand, two additional conditions that should be considered in the selection of electrolytes are the following: ions should be soluble at high salt concentrations and they should be indifferent or inert regarding the colloidal surface. The first condition is related to the

This journal is © the Owner Societies 2016

Phys. Chem. Chem. Phys., 2016, **18**, 21852–21864 | **21861**

experimental fact that the solubility of multivalent electrolytes usually decreases when the valence of ions augments. The second condition is motivated by the experimental observation that there are certain electrolytes and colloidal materials with the property that ions can be adsorbed at the colloidal surface even at the so-called point of zero charge, that is, when the colloids are neutral or uncharged. In general, this ionic adsorption is also dependent on the salt concentration. Ions that are adsorbed onto neutral or uncharged surfaces are said to be "specifically" adsorbed. In the past, this non-coulombic or non-electrostatic interaction has been used in the literature to explain, for example, the sign inversion of the effective colloidal charge that has been detected experimentally as an inversion of the electrophoretic mobility at high salt concentrations of multivalent electrolytes.[60] On the other hand, an inversion of the electrophoretic mobility has also been observed in the presence of indifferent or inert electrolytes (*i.e.*, when short-range "specific" interactions between ions and the colloidal surface can be neglected) *via* electrophoretic mobility experiments.[53] These observations have been explained without the necessity of "specific" short-range interactions *via* theoretical calculations that go beyond the classical Poisson–Boltzmann theory by taking into account ion-correlations, ionic excluded volume effects, and retardation and relaxation contributions.[61,62] We foresee that even if monovalent counterions display some degree of "specific" adsorption onto the colloidal surface, the phenomena of non-dominance of counterions and the non-monotonic order or precedence in the mean electrostatic potential at the Helmholtz plane predicted in this work should be sufficiently robust to be experimentally observable using an appropriate selection of multivalent coions and highly charged colloids. This should be facilitated if (i) the same counterion is used in all electrolytes, (ii) the coions are indifferent regarding the colloidal surface and (iii) they have, approximately, the same ionic size. Also, if the salt is sufficiently concentrated, an order or precedence in the mean electrostatic potential at the Helmholtz plane, the phenomena of charge inversion, local charge reversal, and a local inversion of the electric field near the colloidal surface should be experimentally detectable at low or moderate colloidal surface charge densities as predicted by our theory and simulations.

4 Concluding remarks

The mean electrostatic potential at the Helmoltz plane and the electric field around charged surfaces have been studied here in the presence of monovalent counterions and multivalent coions, when the properties of counterions are the same in all instances. The behaviour of the electrostatic screening at the Helmholtz plane has been analyzed as a function of several parameters such as the valence of coions, the ionic volume fraction, the colloidal surface charge density, and the colloidal geometry. A very important outcome of our simulations and integral equation calculations is that, for equisized z:1 primitive model electrolytes, the properties of the electric double layer do not converge in the limit of very large colloidal surface

charge densities (as the classical Poisson–Boltzmann approach predicts). In other words, it is shown explicitly that, for equally-sized z:1 primitive model electrolytes, counterions do not dominate the properties of the ionic cloud around highly charged colloids when ion correlations and ionic excluded effects are taken into account consistently. These ingredients are missing in classical mean field descriptions, such as the non-linear Poisson–Boltzmann theory, in which counterions determine or dominate asymptotically the behaviour of the electrical double layer in the limit of very high colloidal charges. The present study complements the prior report of the non-dominance of counterions for z:z electrolytes, symmetric in valence and asymmetric in size,[3,5] proving that the non-dominance of counterions is, by no means, an exclusive or direct effect of the ionic size-symmetry. In addition, this survey substantiates the relevance of coions in aqueous electrolyte dispersions of strongly charged colloids at high salt concentrations since, in the classical description of the electric double layer, the size and the valence of coions are irrelevant at high surface charges.

On the other hand, we have shown that the electrostatic screening, measured *via* the mean electrostatic potential at the Helmholtz plane, displays a non-monotonical order or precedence for equally-sized electrolytes that are identical except for the valence and concentration of coions. This order or precedence depends on several parameters such as the valence of coions, the ionic volume fraction of the electrolyte, and the size and charge of the colloid. Based on the planar case, it has been evinced that the occurrence of this phenomenon can be explained in terms of the decay rate of the electric field near the colloidal surface, and by the appearance of a local inversion of the electric field promoted by multivalent coions in the presence of monovalent counterions. In the past, a local inversion of the electric field around charged colloids has been associated with the phenomena of charge inversion and local charge reversal of the bare charge of electrodes or nanoparticles.[43–45] These phenomena have been observed experimentally, for example, in different aqueous colloidal systems containing multivalent counterions.[46–49] To our best knowledge, this is the first time simulations and theoretical calculations predict the occurrence of charge inversion, local charge reversal, and a local inversion of the electric field around charged colloids immersed in aqueous primitive model electrolytes containing only monovalent counterions and multivalent coions, that is in the absence of multivalent counterions and specific ionic short-range attractions. Thus, this new reversible physical mechanism is relevant to promote charge inversion in a manner that is complementary to the widely studied mechanism of charge inversion driven by multivalent counterions or by specific ion adsorption. Notice that the presence of a local charge reversal or charge inversion does not imply necessarily an inversion of the effective charge of a charged colloid,[63] which can be indeed observed experimentally *via* a change of sign in the associated electrophoretic mobility. If the shear plane (where the zeta potential is defined) is located very close to the Helmholtz plane, it could be possible to corroborate the non-monotonic behaviour of the mean electrostatic potential as follows: at very low colloidal surfaces an order or precedence in

the electrophoretic mobility, analogous to the Hofmeister series, should be observed in fine resolution experiments when concentrated salts containing multivalent coions and monovalent counterions are present; under the same electrolyte conditions this order or precedence in the electrophoretic mobility as a function of the coion's valence should be inverted at high colloidal surface charge densities but accesible experimentally.

In terms of possible applications, we would like to mention that the phenomenon of charge inversion promoted by multivalent coions could be useful to promote the self-assembly and trapping/release of small charged nanoparticles, globular proteins, dendrimers or polyelectrolytes at the interface or frontier of highly charged colloidal surfaces with the same sign. These processes can be controlled and fine-tuned by varying the salt concentration and are fully reversible. Given the well-known scarcity of multivalent anions in nature, another appealing application could be to use multivalent cations, instead of multivalent anions, to induce or promote the phenomenon of charge inversion in the presence of positively charged electrodes or cationic colloidal particles. The current mechanism of charge inversion, local charge reversal, and local inversion of the electric field promoted by multivalent coions is general, robust, and probably measurable experimentally. As a result, these phenomena are not restricted to appear only in the spherical and planar geometries studied here, but they should be observed in other geometries (such as the cylindrical geometry) and/or in more complex soft matter systems. We foresee that, under appropriate conditions, the ionic size asymmetry (due to hydration effects) and image charge effects (due to dielectric discontinuities) could enhance significantly the phenomena reported in this study. Such effects could facilitate the experimental observation of the non-dominance of counterions and the non-monotonic order or precedence in the electrostatic screening at the Helmholtz plane, and they could be very useful to ease the implementation of practical applications based on the phenomenon of charge inversion promoted by multivalent coions in concentrated electrolytes with monovalent counterions. Theoretical and simulation work along these lines is currently in progress and will be reported elsewhere.

Acknowledgements

References

1 E. Gonzales-Tovar, M. Lozada-Cassou and D. Henderson, *J. Chem. Phys.*, 1985, **83**, 361.

2 Y. X. Yu, J. Z. Wu and G. H. Gao, *J. Chem. Phys.*, 2004, **120**, 7223.

3 G. I. Guerrero-García, E. González-Tovar, M. Lozada-Cassou and F. J. Guevara-Rodríguez, *J. Chem. Phys.*, 2005, **123**, 034703.

4 L. B. Bhuiyan and C. W. Outhwaite, *Condens. Matter Phys.*, 2005, **8**, 287.

5 G. I. Guerrero-García, E. González-Tovar and M. Chávez-Páez, *Phys. Rev. E: Stat., Nonlinear, Soft Matter Phys.*, 2009, **80**, 021501.

6 G. I. Guerrero-García and M. Olvera de la Cruz, *J. Phys. Chem. B*, 2014, **118**, 8854.

7 E.-Y. Kim and S.-C. Kim, *J. Chem. Phys.*, 2014, **140**, 154703.

8 B. Medasani, Z. Ovanesyan, D. G. Thomas, M. L. Sushko and M. Marucho, *J. Chem. Phys.*, 2014, **140**, 204510.

9 A. Naji, M. Ghodrat, H. Komaie-Moghaddam and R. Podgornik, *J. Chem. Phys.*, 2014, **141**, 174704.

10 E.-Y. Kim, S.-C. Kim, Y.-S. Han and B.-S. Seong, *Mol. Phys.*, 2015, **113**, 871–879.

11 Y. Nakayama and D. Andelman, *J. Chem. Phys.*, 2015, **142**, 044706.

12 C. A. Silvera Batista, R. G. Larson and N. A. Kotov, *Science*, 2015, **350**, 1242477.

13 A. P. dos Santos and Y. Levin, *J. Chem. Phys.*, 2015, **142**, 194104.

14 A. Bakhshandeh, A. P. dos Santos, A. Diehl and Y. Levin, *J. Chem. Phys.*, 2015, **142**, 194707.

15 M. Westbroek, N. Boon and R. van Roij, *Phys. Chem. Chem. Phys.*, 2015, **17**, 25100–25108.

16 M. Ghodrat, A. Naji, H. Komaie-Moghaddam and R. Podgornik, *J. Chem. Phys.*, 2015, **143**, 234701.

17 Z. Ovanesyan, A. Aljzmi, M. Almusaynid, A. Khan, E. Valderrama, K. L. Nash and M. Marucho, *J. Colloid Interface Sci.*, 2016, **462**, 325–333.

18 C. N. Patra, *J. Chem. Eng. Data*, 2015, **60**, 3319–3326.

19 C. P. Kelleher, A. Wang, G. I. Guerrero-García, A. D. Hollingsworth, R. E. Guerra, B. J. Krishnatreya, D. G. Grier, V. N. Manoharan and P. M. Chaikin, *Phys. Rev. E: Stat., Nonlinear, Soft Matter Phys.*, 2015, **92**, 062306.

20 Z.-Y. Wang, *Phys. Rev. E*, 2016, **93**, 012605.

21 C. N. Patra, *Mol. Phys.*, 2016, DOI: 10.1080/00268976.2016.1143126.

22 S. Kewalramani, G. I. Guerrero-García, L. M. Moreau, J. W. Zwanikken, C. A. Mirkin, M. Olvera de la Cruz and M. Bedzyk, *ACS Cent. Sci.*, 2016, DOI: 10.1021/acscentsci.6b00023.

23 J. P. Valleau and G. M. Torrie, *J. Chem. Phys.*, 1982, **76**, 4623.

24 E. A. Barrios-Contreras, E. González-Tovar and G. I. Guerrero-García, *Mol. Phys.*, 2015, **113**, 1190.

25 G. M. Torrie and J. P. Valleau, *J. Phys. Chem.*, 1982, **86**, 3251.

26 S. L. Carnie and G. M. Torrie, *Adv. Chem. Phys.*, 1984, **56**, 141.

27 U. M. B. Marconi, J. Wiechen and F. Forstmann, *Chem. Phys. Lett.*, 1984, **107**, 609.

28 A. F. Khater, D. Henderson, L. Blum and L. B. Bhuiyan, *J. Phys. Chem.*, 1984, **88**, 3682.

This journal is © the Owner Societies 2016

Phys. Chem. Chem. Phys., 2016, **18**, 21852–21864 | **21863**

29 C. W. Outhwaite and L. B. Bhuiyan, *J. Chem. Phys.*, 1986, **84**, 3461.

30 D. Boda, D. H. W. R. Fawcett and S. Sokolowski, *J. Chem. Phys.*, 2002, **116**, 7170.

31 L. Bari Bhuiyan and C. W. Outhwaite, *Phys. Chem. Chem. Phys.*, 2004, **6**, 3467.

32 M. Valiskó, D. Henderson and D. Boda, *J. Phys. Chem. B*, 2004, **108**, 16548.

33 D. Gillespie, M. Valiskó and D. Boda, *J. Phys.: Condens. Matter*, 2005, **17**, 6609.

34 V. Dorvilien, C. N. Patra, L. B. Bhuiyan and C. W. Outhwaite, *Condens. Matter Phys.*, 2013, **16**, 43801.

35 G. I. Guerrero-García, E. González-Tovar and M. Olvera de la Cruz, *J. Chem. Phys.*, 2011, **135**, 054701.

36 G. I. Guerrero-García, P. González-Mozuelos and M. Olvera de la Cruz, *ACS Nano*, 2013, **7**, 9714.

37 C. N. Patra, *RSC Adv.*, 2015, **5**, 25006–25013.

38 E. González-Tovar and M. Lozada-Cassou, *J. Phys. Chem.*, 1989, **93**, 3761.

39 G. M. Torrie and J. P. Valleau, *J. Chem. Phys.*, 1980, **73**, 5807–5816.

40 D. Boda, K. Chan and D. Henderson, *J. Chem. Phys.*, 1998, **109**, 7362–7371.

41 L. Blum, *Mol. Phys.*, 1975, **30**, 1529.

42 K. Hiroike, *Mol. Phys.*, 1977, **33**, 1195.

43 G. I. Guerrero-García, E. González-Tovar and M. Olvera de la Cruz, *Soft Matter*, 2010, **6**, 2056.

44 G. I. Guerrero-García and M. Olvera de la Cruz, *J. Chem. Theory Comput.*, 2013, **9**, 1–7.

45 G. I. Guerrero-García, Y. Jing and M. Olvera de la Cruz, *Soft Matter*, 2013, **9**, 6046–6052.

46 E. Raspaud, I. Chaperon, A. Leforestier and F. Livolant, *Biophys. J.*, 1999, **77**, 1547–1555.

47 K. Besteman, M. A. G. Zevenbergen, H. A. Heering and S. G. Lemay, *Phys. Rev. Lett.*, 2004, **93**, 170802.

48 M. Quesada-Pérez, E. González-Tovar, A. Martín-Molina, M. Lozada-Cassou and R. Hidalgo-Álvarez, *Colloids Surf., A*, 2005, **267**, 24–30.

49 F. H. J. van der Heyden, D. Stein, K. Besteman, S. G. Lemay and C. Dekker, *Phys. Rev. Lett.*, 2006, **96**, 224502.

50 S. M. Ahmed, *J. Phys. Chem.*, 1969, **73**, 3546–3555.

51 V. Peyre, O. Spalla, L. Belloni and M. Nabavi, *J. Colloid Interface Sci.*, 1997, **187**, 184–200.

52 M. Quesada-Pérez, E. González-Tovar, A. Martín-Molina, M. Lozada-Cassou and R. Hidalgo-Álvarez, *ChemPhysChem*, 2003, **4**, 234–248.

53 M. Elimelech and C. R. O'Melia, *Colloids Surf.*, 1990, **44**, 165–178.

54 Y. Marcus, *Chem. Rev.*, 1988, **88**, 1475–1498.

55 F. Vereda, A. Martín-Molina, R. Hidalgo-Álvarez and M. Quesada-Pérez, *Phys. Chem. Chem. Phys.*, 2015, **17**, 17069–17078.

56 K. D. Danov, E. S. Basheva and P. A. Kralchevsky, *Materials*, 2016, **9**, 145.

57 M. M. Kohonen, M. E. Karaman and R. M. Pashley, *Langmuir*, 2000, **16**, 5749–5753.

58 F. J. M. Ruiz-Cabello, M. Moazzami-Gudarzi, M. Elzbieciak-Wodka, P. Maroni, C. Labbez, M. Borkovec and G. Trefalt, *Soft Matter*, 2015, **11**, 1562.

59 T. Cao, I. Szilagyi, T. Oncsik, M. Borkovec and G. Trefalt, *Langmuir*, 2015, **31**, 6610–6614.

60 I. Semenov, S. Raafatnia, M. Sega, V. Lobaskin, C. Holm and F. Kremer, *Phys. Rev. E: Stat., Nonlinear, Soft Matter Phys.*, 2013, **87**, 022302.

61 M. Lozada-Cassou, E. González-Tovar and W. Olivares, *Phys. Rev. E: Stat. Phys., Plasmas, Fluids, Relat. Interdiscip. Top.*, 1999, **60**, R17.

62 M. Lozada-Cassou and E. González-Tovar, *J. Colloid Interface Sci.*, 2001, **239**, 285–295.

63 B. Luan and A. Aksimentiev, *Soft Matter*, 2010, **6**, 243–246.